Geometry-induced asymmetric diffusion

Robert S. Shaw*†, Norman Packard*‡§, Matthias Schröter¶, and Harry L. Swinney†¶

*ProtoLife, Via della Libertá 12, 30175 Venezia, Italy; ‡European Center for Living Technology, S. Marco 2847, 30124 Venezia, Italy; §Santa Fe Institute, 1399 Hyde Park Road, Santa Fe, NM 87501; and ¶Center for Nonlinear Dynamics and Department of Physics, University of Texas, Austin, TX 78712

Contributed by Harry L. Swinney, April 18, 2007 (sent for review February 26, 2007)

Past work has shown that ions can pass through a membrane more readily in one direction than the other. We demonstrate here in a model and an experiment that for a mixture of small and large particles such asymmetric diffusion can arise solely from an asymmetry in the geometry of the pores of the membrane. Our deterministic simulation considers a two-dimensional gas of elastic disks of two sizes diffusing through a membrane, and our laboratory experiment examines the diffusion of glass beads of two sizes through a metal membrane. In both experiment and simulation, the membrane is permeable only to the smaller particles, and the asymmetric pores lead to an asymmetry in the diffusion rates of these particles. The presence of even a small percentage of large particles can clog a membrane, preventing passage of the small particles in one direction while permitting free flow of the small particles in the other direction. The purely geometric kinetic constraints may play a role in common biological contexts such as membrane ion channels.

asymmetric pores | channels

Asymmetric diffusion appears in studies of ion transport across membranes (1–12), and in the context of osmosis (13, 14). Ion pores in biological membranes often act as effective rectifiers, blocking the passage of a particular ion in one direction while allowing free flow in the other. Explanations of these phenomena emphasize electrostatic effects or conformational changes. For example, a blocking ion might pass part way through a membrane pore and then become bound, preventing passage of subsequent ions. If the pore is asymmetric, the membrane can act as a rectifier. Here, we demonstrate that asymmetric diffusion can occur with no ionic binding, in a fixed pore geometry. Blocker particles can be held in place by purely geometrical and kinetic constraints, even though particles are in rapid random motion.

We present both a laboratory experiment and a computer simulation to demonstrate this effect. In the experiment, macroscopic (1 mm) glass beads diffuse through a metal asymmetric membrane, and random motions are generated by rapidly vibrating the container. In the simulation, a two-dimensional gas of elastic hard disks of different sizes diffuses through an asymmetric membrane. In both cases, nearly complete rectification is easily demonstrated.

Results

Simulations. Fig. 1 shows typical snapshots from the hard disk gas simulation. In both panels the gas is initially restricted to the right chamber and then tends toward equilibrium as the smaller disks move from right to left through the membrane. However, in the lower panel, the larger disks soon clog the pores and greatly reduce the rate of diffusion of the smaller disks through the membrane. The presence of the smaller disks bombarding the larger disks within the pore makes it highly unlikely that the larger disks will be able to emerge from the pore. Fig. 2 displays the concentration in the left chamber as a function of time for both orientations of the membrane. The flow entering from the smaller end of the pores (Fig. 1*A*) behaves as if there were a well defined fixed diffusion constant, but the flow through the membrane that enters the larger end of the pores (Fig. 1*B*) drops to near zero, as the membrane seals itself. The clogging behavior of this direction of flow is maintained even at lower concentrations of large disks. The number of disks in the plateau region may vary from run to run, depending on how many small disks are able to cross before the membrane seals.

The simulated model is a purely energy-conserving Hamiltonian system, yet it can relax to a long-lived macroscopic state of disequilibrium, with two subsystems at different temperatures. The more rapidly moving disks preferentially pass through the membrane, resulting in a higher temperature on the left side. Such a temperature difference is typical of an effusion process (15). There is a very slow equalization of temperature through collisions at the small ends of the pores, and of concentration through the occasional unblocking of a pore due to fluctuations, but the disequilibrium can persist for very long times.

Experiments. The experiment has two species of glass beads that correspond to the two species of disks in the simulation, and a brass membrane with asymmetric pores, as illustrated in Fig. 3. The results from experiment are qualitatively the same as those from simulation (Fig. 2). Once again, there is free flow through the membrane from the side with the small pore ends, and clogging for flow in the other direction. Fig. 2 *Inset* shows that the number of small beads passing through the membrane before it clogs can again vary from run to run. The clogging is not permanent. Runs longer than 30 min show a leak rate of $\approx$0.1 bead per minute per pore, for this number of beads.

Fig. 4 shows the effect of membrane thickness on the blocking effect. For the thinnest membrane, there is no blocking effect, and the flow is even enhanced in the funneled direction. This is in accord with the single-species small bead experiment mentioned below. The membrane must be of a minimum thickness to produce a significant backing-up of the blocking beads. If there is a large concentration gradient across the pore, the blocking beads will be held in place by this gradient. The backing-up requirement is central to the effect.

When only small beads are present in the experiment, there is a bias in the dynamics, as Fig. 5 illustrates. The small beads pass more readily through the membrane when they enter the large end of the pores, and the system approaches a dynamic equilibrium with more beads on the side with the small pore ends. This asymmetry can be explained by the dissipative nature of the particle-wall collisions, which reduces the normal component of the colliding particle; therefore, the angle between the particle velocity vector and the sidewall becomes smaller (16). In this way the collisions inside the large end of the pore focus a particle trajectory toward the small end of the pore and therefore increase the effective "cross section."

Leaky Membrane Simulation Results. Some insight into the dynamics of the hard disk system can be garnered by considering the

Author contributions: R.S.S., N.P., M.S., and H.L.S. designed research; R.S.S. and N.P. performed research; R.S.S., N.P., M.S., and H.L.S. analyzed data; and R.S.S., N.P., M.S., and H.L.S. wrote the paper.

The authors declare no conflict of interest.

Freely available online through the PNAS open access option.

†To whom correspondence may be addressed. E-mail: rob@protolife.net or swinney@chaos.utexas.edu.

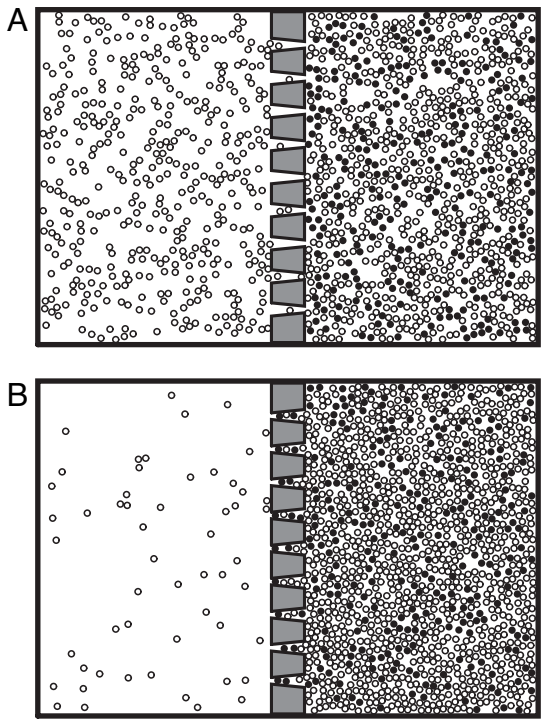

Fig. 1. Snapshots of a binary mixture of hard sphere disks, initially all on the right side, that diffuse through an asymmetric membrane whose pores are smaller on the right end in *A* and on the left end in *B*. Flow through the membrane is highly reduced with the membrane geometry of *B*. The larger particles in the gas mixture are slightly too large to pass through the pores, and the smaller particles are just small enough to pass. The left chamber is initially empty, and the elapsed time is the same for *A* and *B*.

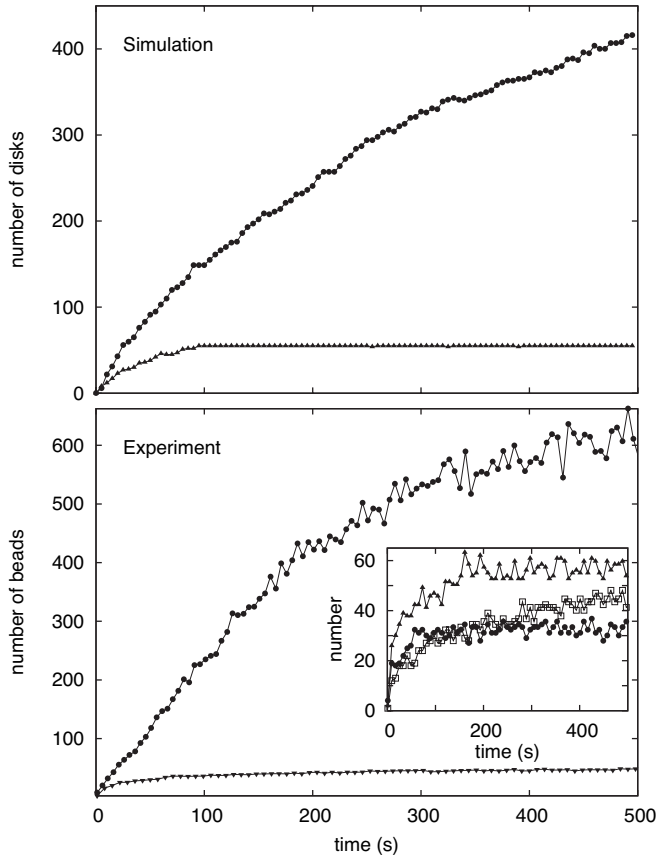

Fig. 2. Number of particles in the (initially empty) left-hand chamber (cf. Fig. 1) in simulation and experiment. In each graph, the upper curve corresponds to pores with their small end on the right, and the lower curve corresponds to the reverse orientation of the pores. The upper curves show a large diffusion rate (slope of the curves), whereas the lower curves illustrate that the pores rapidly clog and the diffusion rate approaches zero. (*Inset*) Clogging for three different experimental trials. The right-hand chamber initially had 1,350 disks in the simulation and 2,000 beads in the experiment, which used a membrane of thickness 9.53 mm; the data shown are an average of three experiments. In both cases, 20% of the particles were large and the remainder were small.

response to an imposed variation in the number of small particles in the chamber on the membrane side with the small pores (left side in Fig. 1*B*). The resultant macroscopic state of the chamber on the right side, which we will call the "inside," shows a path dependence, as illustrated in Fig. 6. Initially, the system had 200 large particles in the inside (right) chamber and no large particles on the outside (left) chamber; initially, no small particles were in either chamber. In Fig. 6*A*, the number of small disks in the outside chamber is gradually increased at a rate of two disks per time unit, up to 1,200 disks. Each disk is added with unit speed, at a random position and moving in a random direction. The number of small disks on the inside chamber can be seen to follow this increase, as one would expect from a simple diffusion process. Then, the number of small disks on the outside is reduced at the same slow rate, and again the disks on the inside roughly follow. When there is no strong concentration gradient across the membrane, the pores conduct freely in both directions.

In Fig. 6*B*, the number of small disks in the outside chamber is again increased at a rate of two disks per time unit up to 1,200 disks, and then this time the number of disks on that side is suddenly reduced to zero; any small disks leaking through from the inside to the outside are removed from the system. In this case, the instantaneous formation of a large concentration gradient across the membrane causes it to clog, and diffusion from the inside initially drops to nearly zero, even though the final concentration outside is the same as in Fig. 6*A*.

The diffusion outward does not, however, remain at zero, because the initial concentration of blocker disks inside is small enough so that there is a significant leakage current. Each small step in the descending portion of the curve in Fig. 6*B* corresponds to a single pore opening for a time; a large blocker disk is dislodged by a fluctuation, and a "patch clamp" observation of that pore would show a current of small disks flowing outward until the pore is resealed by another large disk entering it. Eventually, the concentration of small disks on the right becomes too small to maintain the clogged membrane, and the concentration curve on the right returns to a simple diffusive decrease. Because there are only nine pores in this simulation, the length of the plateau corresponding to the clogging is variable, but the general shape of the knee is repeatable.

The possible biological relevance of this clogging effect to membrane rectification is evident. Possibly, the simple rectification described here could have played a role in tide-pool scenarios of the origin of life. In our simulation, repeated sawtooth driving on the outside will maintain a concentration gradient indefinitely, even with a leaky membrane. Similarly, one can imagine that repeated evaporation and flooding of a primeval tide-pool may have provided the conditions for a sustained gradient across the membrane of an early vesicle, enough to drive a protometabolism (17).

Discussion

If flows across a membrane are governed by the ordinary diffusion equation, they will reverse exactly, if the concentration gradient across the membrane is reversed, regardless of the geometry of the pores. Implicit in the use of the linear diffusion equation is the

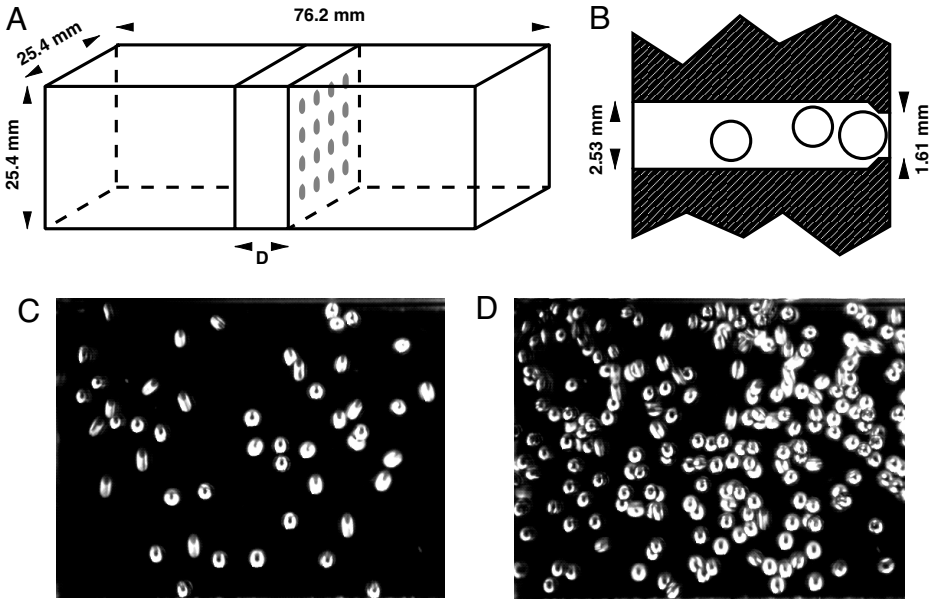

Fig. 3. The experimental system and pictures of the granular gas. (*A*) Diagram of the experimental setup. (*B*) Cross-section of a circular pore that has a reduced diameter on the right end, too small for the larger particles in the binary mixture to pass. (*C*) Side view image of 50 beads in a chamber. (*D*) Side view image of 250 beads in a chamber.

point-particle assumption. Particles do not interact, and solutions to the equations of motion are the same up to a factor for a dense gas or a dilute gas, both in the bulk and in the pore.

If the diffusing particles have a size comparable to the pores through which they are moving, the linear diffusion equation is no longer applicable. In the dilute limit, flows will still be symmetric under reversal of the concentration gradient, for any pore shape. But when concentrations are raised and particles interact with each other and the walls of an asymmetric pore, the symmetry is broken, and the diffusion rates from one side or the other can differ.

Flux ratio theorems indicating a symmetry in diffusion across membranes have been proven for a variety of systems, e.g., with linear intramembrane trapping kinetics for the diffusing particles (18, 19) and even for multicomponent systems such as the one studied here (20). However, these theorems fail here because the trapping kinetics do not include the kinetic constraints felt by the spatially extended particles interacting with pores.

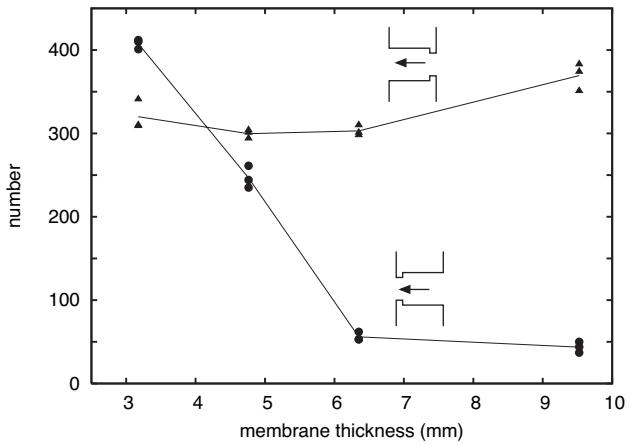

Fig. 4. Number of small beads measured to cross the membrane after 3 min, as a function of membrane thickness, for the two flow directions (cf. Fig. 3). The loaded side of the membrane initially had a mixture of 1,600 small beads and 400 large beads.

At first examination, asymmetric diffusion might seem counterintuitive, at odds with the Second Law. But there is no contradiction, because this is a nonequilibrium effect, being driven here by increased concentration on one side. At equilibrium, detailed balance will hold, and we expect fluctuations around equilibrium to be symmetric. However, a clogged membrane is held away from equilibrium, in a long-lived metastable state. A concentration gradient across the pore is required to keep blocking particles in place, but this gradient can be made arbitrarily small by lengthening the pore.

Asymmetric diffusion could be relevant to biological situations; rectification can be generated in isothermal conditions, driven by only a small concentration gradient. Asymmetry has long been noted in movements of ions through channels in membranes, where the asymmetry is often described as a form of rectification (1). Although ion channels can be complicated devices, with voltage sensors and internal conformational changes, a particularly simple pore design is the inward-rectifier potassium channel [for a review, see Lu (21)]. Early modeling of this channel described the outward flow of K^+ ions through the channel as being blocked by larger ions, which are present on the inside of the cell and cannot pass completely through (22–25). Recent detailed imaging (26) of a potassium channel shows an asymmetric pore, narrow toward the outside and wider toward the inside, roughly like our model pores represented in Figs. 3*B* and 1.

The early rectification models of Hille and Schwartz (23) explicitly included the requirement that a blocker back out of the channel to reenable flow. However, these and other models emphasize electrical effects, in particular intrapore binding sites, to keep the blockers in place in the pore. Electrostatic interactions among ions and possible binding sites will of course be very important, but we have demonstrated that an asymmetric geometry alone can also lead to rectification. We suggest that the clogging effect described in this article could play a role in maintaining blocking and rectification. The inclusion of this effect may help clarify discussions of ''multiion channels'' (23, 27). Geometry-induced asymmetric diffusion could occur in any physical context that includes the interaction of shapes in restrictive geometries, as exemplified by our experiment and its

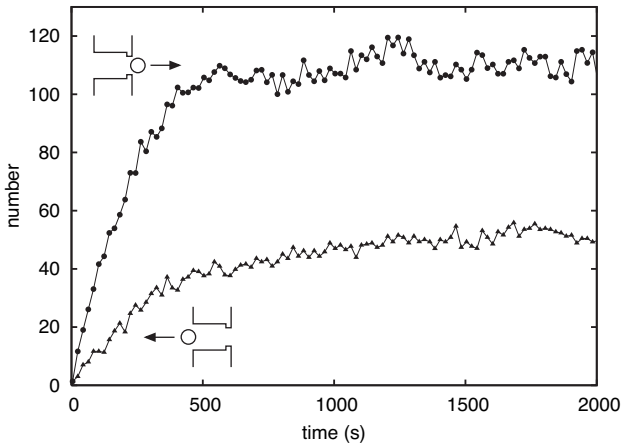

Fig. 5. Number of beads measured to pass through a membrane (9.53 mm thick), as a function of time, when only small beads were present. Flow in the direction from the large to the small end of the pores is enhanced relative to that for the reverse orientation of the pores. There was a total of 200 beads; those residing in the pores were not observed.

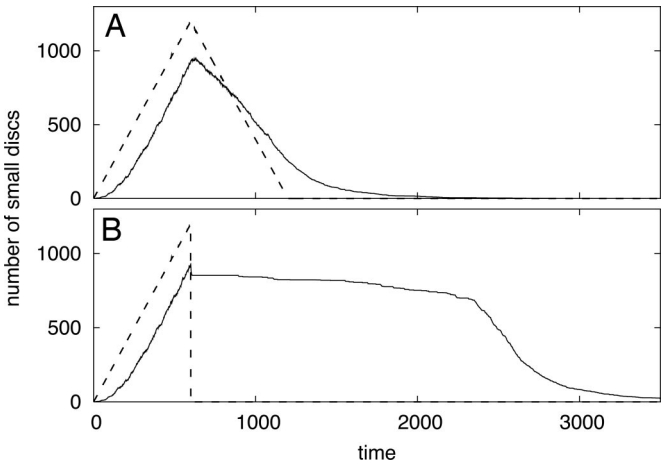

Fig. 6. Time-dependent variation of concentration of small disks (solid lines) in the chamber on the right (the ''inside'') in Fig. 1*B*, in response to variation of number of small disks in the left-hand (''outside'') chamber (dashed lines). The number of large disks in the inside chamber is 200, and the number of large disks in the outside chamber is zero. (*A*) When the number of disks outside is linearly increased to 1,200 and then decreased linearly at the same rate, the number of disks on the inside adiabatically follows. (*B*) When the number of small disks outside is linearly increased as in *A* and then suddenly decreased to zero, the membrane pores clog as a consequence of the sudden strong cross-membrane gradient, and the number of small particles on the inside remains nearly constant for a long time.

membrane model. It is natural for large objects to get stuck and to block passage of following objects; all that is required is a certain density and a flow direction, no matter how small the flow. The simplicity of the conditions generating the effect suggests that it might occur quite commonly in biological systems, where membranes are ubiquitous, and molecules of all shapes and sizes are closely packed (28). Large changes in forward and backward diffusion rates can be effected by small changes in pore geometry, or object shape. The simple clogging phenomenon arising from asymmetric pores suggests a possible evolutionary path from a purely mechanical rectification that might occur in a prebiotic vesicle, to the sophisticated membrane ion channels present in living systems today.

Materials and Methods

Experiment. A parallelepiped container is made of standard microscope slides for the top and sides, and cut slides for the ends. The bottom of the container is brass with the interior surface machined with a pattern of 2-mm-wide divots to deflect beads from vertical motion, to help randomize the motion. The container is divided into two chambers by a brass membrane whose thickness D was varied (Fig. 3*A*). Each membrane has 16 circular pores with a long large-diameter section (whose length depends on the membrane thickness) and a concentric short small-diameter constriction (whose length is fixed at 1 mm), as shown in Fig. 3*B*.

Particles of two different sizes are obtained by repeated sieving of soda lime glass beads (sphericity >95%) with a broad size distribution (Ceroglass GSR). The ''large'' beads (average mass of 7.6 mg) have diameters of 1.70–1.85 mm, small enough to fit into the large-diameter end of a membrane pore but too large to pass through the narrow end of a pore. The ''small'' beads (average mass of 4.2 mg) have diameters of 1.40–1.55 mm, small enough so that they can easily pass completely through the pores but large enough so that they have to stay in single file in the large-diameter portion of the pore (see Fig. 3*B*).

In each run the chamber on one side of the membrane is loaded with beads, and then the container is oscillated vertically at 30 Hz with an acceleration amplitude $9.5g$ (g is the gravitational acceleration). To the eye, the bead motion is vigorous and random. Pictures such as those in Fig. 3 *C* and *D* are taken at 1-sec intervals (1/2,000 sec exposure time) with a digital imaging system (Kodak Motion Corder Analyzer SR 1000) synchronized with the driving frequency.

The number of small beads passing through the membrane into an initially empty chamber was counted as a function of time by using an image processing algorithm that is accurate to within one or two beads for up to ≈80 beads, as in Fig. 3*C*. For a larger number of beads, as in Fig. 3*D*, the algorithm undercounts the number of beads because of eclipsing and grouping effects, but a correction factor obtained by weighing the beads and checked by direct hand counting yields counts accurate to 5%.

Hard Disk Simulation. The simulation uses a two-dimensional container divided by a membrane into two chambers, each 3 units high by 2 units wide, as shown in Fig. 1. The membrane has nine tapered pores, 0.04 units wide on the large end and 0.02 units wide on the small end. There are two species of elastic hard disks, ''small'' disks (diameter of 0.018) and ''large'' disks (diameter of 0.022). As in the experiment, the small disks can pass through the pores in either direction, whereas the large disks cannot pass through the narrow end of a pore. There are initially 1,350 disks on the right side, 20% of which are the large disks; the left side is initially empty.

All disks have the same mass and have initial unit velocities uniformly distributed in random directions. A period of at least 10 time units is allowed to pass before the pores are opened, to allow the velocity distributions to thermalize; each simulation is subsequently run for 500 time units. The work of Forster *et al.* (29) shows that the dynamical entropy of such systems is high, so that the Maxwellian distribution is rapidly achieved and preserved even in very restrictive geometries.

We thank Josh Deutsch for a critical reading of the manuscript and Mark Bedau, Jim Bredt, Jim Crutchfield, Robert S. Eisenberg, Doyne Farmer, Kristian Lindgren, and John McCaskill for helpful comments. R.S.S. and N.P. appreciate the hospitality of the Santa Fe Institute and the European Center for Living Technology. The experiments were conducted at the University of Texas with the support of the Sid Richardson Foundation. This work was partially funded by Programmable Artificial Cell Evolution, the Information Society as a Complex System project, European Union Projects FP5 and FP6, and the IST-FET Complex Systems Initiative.

1. Hille B (2001) *Ion Channels of Excitable Membranes* (Sinauer, Sunderland, MA).
2. Chen DP, Eisenberg RS (1993) *Biophys J* 65:727–746.
3. Siwy Z, Fuliński A (2002) *Phys Rev Lett* 89:198103.
4. Siwy Z, Kosińska ID, Fuliński A, Martin CR (2005) *Phys Rev Lett* 94:048102.
5. Siwy ZS, Powell MR, Kalman E, Astumian RD, Eisenberg RS (2006) *Nano Lett* 6:473–477.
6. Kosińska ID, Fuliński A (2005) *Phys Rev E* 72:011201.
7. Kosztin I, Schulten K (2004) *Phys Rev Lett* 93:238102.
8. Cervera J, Schiedt B, Ramírez P (2005) *Europhys Lett* 71:35–41.
9. Cervera J, Schiedt B, Neumann R, Mafé S, Ramírez P (2006) *J Chem Phys* 124:104706.
10. Bauer WR, Nadler W (2006) *Proc Natl Acad Sci USA* 103:11446–11451.
11. Smeets RMM, Keyser UF, Krapf D, Wu MY, Dekker NH, Dekker C (2006) *Nano Lett* 6:89–95.
12. Kolomeisky AB (2007) *Phys Rev Lett* 98:048105.
13. Chou T (1999) *J Chem Phys* 110:606–615.
14. Kim KS, Davis IS, Macpherson PA, Pedley TJ, Hill AE (2005) *Proc R Soc London Ser A* 461:273–296.
15. Cleuren B, Van den Broeck C, Kawai R (2006) *Phys Rev E* 74:021117.
16. Brilliantov NV, Pöschel T (2004) *Kinetic Theory of Granular Gases* (Oxford Univ Press, Oxford).
17. Chen I, Szostak JW (2004) *Proc Natl Acad Sci USA* 101:7965–7970.
18. Sten-Knudsen O, Ussing HH (1981) *J Membr Biol* 63:233–242.
19. Bass L, Bracken AJ, Hilden J (1986) *J Theor Biol* 118:327–338.
20. McNabb A, Bass L (1990) *IMA J Appl Math* 44:155–161.
21. Lu Z (2004) *Annu Rev Physiol* 66:103–129.
22. Armstrong CM, Binstock L (1965) *J Gen Physiol* 48:859–872.
23. Hille B, Schwartz W (1978) *J Gen Physiol* 72:409–442.
24. Vandenberg CA (1987) *Proc Natl Acad Sci USA* 84:2560–2564.
25. Matsuda H, Saigusa A, Irisawa H (1987) *Nature* 325:156–159.
26. Doyle DA, Cabral JM, Pfuetzner RA, Kuo A, Gulbis JM, Cohen SL, Chait BT, MacKinnon R (1998) *Science* 280:69–77.
27. Lester HA, Dougherty DA (1998) *J Gen Physiol* 111:181–183.
28. Goodsell DS (1993) *The Machinery of Life* (Springer, New York).
29. Forster Ch, Mukamel D, Posch HA (2004) *Phys Rev E* 69:066124.